INFORMATICA, 2011, Vol. 22, No. 3, 383–394

Separable Image Denoising Based on the Relative Intersection of Confidence Intervals Rule

Jonatan LERGA, Victor SUCIC, Miroslav VRANKIĆ

Faculty of Engineering, University of Rijeka
Vukovarska 58, HR-51000 Rijeka, Croatia
e-mail: jlerga@riteh.hr, vsucic@riteh.hr, mvrankic@riteh.hr

Received: April 2009; accepted: November 2010

Abstract. In this paper we have proposed a novel method for image denoising using local polynomial approximation (LPA) combined with the relative intersection of confidence intervals (RICI) rule. The algorithm performs separable column-wise and row-wise image denoising (i.e., independently by rows and by columns), combining the obtained results into the final image estimate. The newly developed method performs competitively among recently published state-of-the-art denoising methods in terms of the peak signal-to-noise ratio (PSNR), even outperforming them for small to medium noise variances for images that are piecewise constant along their rows and columns.

Keywords: relative intersection of confidence intervals (RICI) rule, image restoration, image denoising, adaptive filters, adaptive signal processing.

1. Introduction

Noise appears in almost all real images due to imperfections of image acquisition systems. That is why image denoising is one of the fundamental problems in the field of image processing, needed for improving image quality before performing different high-level vision tasks (e.g., object detection (Serackis *et al.*, 2010), image completion (Wu *et al.*, 2010), etc.). Consequently, various denoising methods have been proposed, many of which can be found in Buades *et al.* (2004) where their characteristics are described and compared. A brief overview of image denoising methods is given in Section 2.

However, each of those methods has its advantages, as well as the limitations (for example the type of the images when a particular method performs best). The main objective of this paper is to develop an improved denoising method for a class of piece-wise constant images, the model of which was given in Ausbeck (2000). The proposed method is then compared to several newly developed hybrid methods which combine two or more existing methods, such as for example the recently proposed shape adaptive DCT (SA-DCT) method (Foi and Egiazarian, 2007), the block-matching and 3D filtering (BM3D) algorithm (Dabov *et al.*, 2007), or the method that combines the intersection of confidence intervals (ICI) rule (Katkovnik *et al.*, 2004) and local polynomial approximation (LPA-ICI) for spatially adaptive image restoration (Katkovnik *et al.*, 2004). The SA-DCT

method is based on the ICI rule (Katkovnik, 1999) and it uses arbitrarily-shaped 2D supports which are adapted with respect to the image features, hence reducing unwanted artifacts in the image. The BM3D algorithm uses 2D image fragments and groups them into 3D data, resulting in the improved sparse representation of the image in the transform domain. In addition, collaborative Wiener filtering leads to further improvements in denoised image. In the anisotropic implementation of the LPA-ICI, LPA is used in designing kernels with a desirable polynomial smoothness, while the ICI rule results in adaptive varying scales of the kernel estimates.

Unlike the above mentioned methods, the method proposed in this paper is based on 1D filtering that is locally tuned to the signal (image) according to the improved ICI rule – the relative intersection of confidence intervals (RICI) rule (Lerga *et al.*, 2008). The RICI rule is combined with local polynomial approximation (LPA), hence allowing to have an adaptive data-driven LPA-based filter for each image pixel. The 1D filtering along image rows and columns makes the proposed method computationally more efficient than its two-dimensional counterparts.

The paper is organized as follows. Section 2 gives the summary of existing image denoising techniques. In Section 3 the RICI rule is briefly outlined. The proposed denoising algorithm based on the RICI rule is described in Section 4. Section 5 presents the experimental results for different test images, and gives a comparison of the proposed method and other popular image denoising techniques.

2. A Brief Review of Image Denoising Methods

Image denoising methods can be divided, as in Motwani *et al.* (2004), into two main groups: spatial filtering methods and transform domain filtering methods.

Spatial filtering methods can be linear (as, for example, the one using the Wiener filtering) or non-linear (such as low filtering methods or various spatial filtering methods using median filters).

The transform domain filtering methods are categorized as either adaptive (for example, independent component analysis (ICA) method) or non-adaptive methods (as spatial-frequency filtering and wavelet domain filtering methods). The ICA method was proposed for the case of non-Gaussian noise. However, it is time consuming, as it is the spatial-frequency filtering method based on the fast Fourier transform which is highly affected by the selected cut-off frequency and the filter design.

As in Motwani *et al.* (2004), the wavelet based image denoising methods can be categorized as linear filtering methods (such as the one using the Wiener filter in the wavelet domain, which is optimal in terms of the mean square error for images corrupted by Gaussian noise), non-linear threshold filtering (which apply hard or soft thresholding with the threshold chosen using different adaptive or non-adaptive methods), non-orthogonal wavelet transforms methods (including undecimated wavelet transform, shift invariant discrete wavelet transform and multiwavelets) and wavelet coefficient model methods (which can be deterministic or statistical). The statistical wavelet coefficient models can

be further classified as marginal probabilistic model and joint probabilistic model methods.

However, during the last decades various hybrid methods which combine wavelet based methods and some other image processing techniques were developed, such as the one proposed in Tomic *et al.* (2008) which uses the ICI rule for adaptive wavelet support selection.

Here proposed method can be classified as a spatial filtering image denoising method, using the improved ICI rule (called the RICI rule) as the tool for the adaptive filter support size selection and the LPA for the filter design.

3. The RICI Rule

For the purpose of signal denoising, in this paper we have used LPA-based filters. For each signal sample, the LPA filter with the appropriate support is chosen using the RICI rule (Lerga *et al.*, 2008). The RICI rule allows us to choose filters with long supports in smooth signal regions, and short supports near signal discontinuities. For that purpose, a set of LPA based filters of growing supports is applied to each signal sample, resulting in a set of estimates of the noise-free sample value.

The RICI rule chooses the estimate which gives the best compromise between the estimation bias and variance. This choice is based on tracking the intersection of confidence intervals of estimates $\hat{x}_{l(k)}(n)$ obtained for growing filter supports with length $l(k)$, where k stands for the filter support index and n is the signal sample index. The largest lower and the smallest upper limit of the confidence intervals are respectively defined as:

$$\bar{L}(n,k) = \max_{i=1,\ldots,k}[\hat{x}_{l(k)}(n) - \Gamma\sigma_{l(k)}(n)], \tag{1}$$

$$\underline{U}(n,k) = \min_{i=1,\ldots,k}\left[\hat{x}_{l(k)}(n) + \Gamma\sigma_{l(k)}(n)\right], \tag{2}$$

where $\sigma_{l(k)}$ is the standard deviation of the estimation error, and Γ is the confidence level of the confidence intervals. The number of filter taps is chosen as the largest one for which it is still true that:

$$\bar{L}(n,k) \leqslant \underline{U}(n,k), \tag{3}$$

and

$$R(n,k) \geqslant R_c, \tag{4}$$

where $R(n,k)$ is the ratio of the size of the intersection of all confidence intervals obtained so far and the size of the current confidence interval, that is:

$$R(n,k) = \frac{\underline{U}(n,k) - \bar{L}(n,k)}{2\Gamma\sigma_{l(k)}(n)}. \tag{5}$$

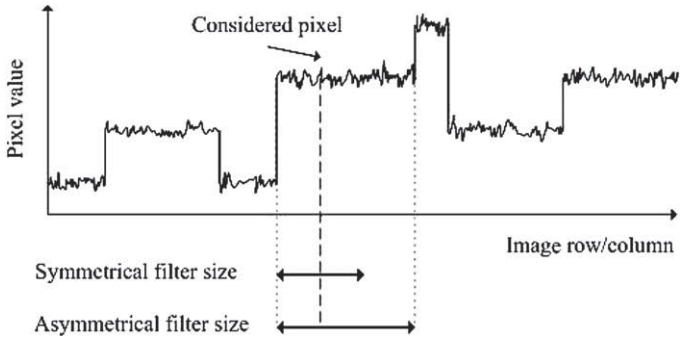

Fig. 1. Example of symmetrical and asymmetrical filter support selection.

The parameter R_c in (4) is empirically chosen, as described in Lerga *et al.* (2008).

An advantage of the proposed algorithm, as well as the original ICI rule, is that it requires only the knowledge of the noise variance σ_n^2 and not the estimation of the bias, which is needed by other methods based on asymptotic formulae where the optimal filter support is defined as a function of both the bias and the variance; see for example Fan and Gijbels (1996) and Ruppert (1997).

The proposed LPA-RICI method, unlike the LPA-ICI method, allows us to select larger Γ and so achieve better estimation accuracy in terms of the peak signal-to-noise ratio (PSNR) by selecting the appropriate R_c value (Lerga *et al.*, 2008). In the case of LPA-ICI, a larger Γ results in wider confidence intervals, as it can be observed from (1) and (2), hence resulting into signal oversmoothing due to the longer filter support. This problem is avoided with the additional criterion (4) which ensures that the most appropriate filter support is selected.

We have used asymmetrical filter supports by allowing them to grow independently both to the left-hand and to the right-hand side from the estimated sample, hence giving us a more accurate estimate of the denoised signal. The Fig. 1 shows a sketch of a noisy image row/column, and a difference between symmetrical and asymmetrical filter support selection for one pixel. Estimating the noise-free pixel value using the asymmetrical filter support (for example as the mean value of the selected region) results in better noise suppression than for the case when the symmetrical filter support is used. This is a result of the central limit theorem whereby the lager number of samples (the asymmetrical region) results in an estimate closer to the true value and thus in better noise elimination.

4. Image Denoising Algorithm

Let us consider a noisy image $y(i,j)$, obtained as:

$$y(i,j) = x(i,j) + n(i,j), \tag{6}$$

where $x(i,j)$ is the clean image and $n(i,j)$ is zero-mean additive white Gaussian noise (AWGN) with the variance σ_n^2.

Let us also define operators H_r and H_c which perform row-wise and column-wise image denoising, respectively. Each operator uses the 1D adaptive data-driven LPA based filter whose support is determined by the RICI rule, explained above, for each signal sample.

The algorithm consists of three stages:

First stage: The operator H_r is applied to the noisy image $y(i,j)$, resulting in the image $\hat{x}_r(i,j)$:

$$\hat{x}_r(i,j) = H_r\big\{y(i,j)\big\}. \tag{7}$$

Next, the operator H_c is applied to $\hat{x}_r(i,j)$ resulting in the image $\hat{x}_{rc}(i,j)$:

$$\hat{x}_{rc}(i,j) = H_c\big\{\hat{x}_r(i,j)\big\}. \tag{8}$$

Second stage: In this stage of the algorithm, the order of the operators H_r and H_c is reversed. The operator H_c is used first, giving the image $\hat{x}_c(i,j)$:

$$\hat{x}_c(i,j) = H_c\big\{y(i,j)\big\}. \tag{9}$$

Then, the operator H_r is applied to $\hat{x}_c(i,j)$ resulting in the image $\hat{x}_{cr}(i,j)$:

$$\hat{x}_{cr}(i,j) = H_r\big\{\hat{x}_c(i,j)\big\}. \tag{10}$$

Note that the first and the second stage of the algorithm are performed in parallel, which significantly speeds up its execution time. Since the operators H_r and H_c simultaneously denoise each row and column respectively, an additional reduction in the computation time is also achieved. A more detailed study of the ICI method complexity can be found in Katkovnik *et al.* (2006).

Third stage: The final image estimate is obtained as a weighted sum of the results from the previous two stages:

$$\hat{x}(i,j) = w_{rc}(i,j)\cdot\hat{x}_{rc}(i,j) + w_{cr}(i,j)\cdot\hat{x}_{cr}(i,j), \tag{11}$$

where $w_{rc}(i,j)$ and $w_{cr}(i,j)$ denote weighting factors. Here we will consider two sets of the weights. In the first case, the weighting factors are chosen as $w_{rc}(i,j) = w_{cr}(i,j) = 0.5$. In the second case, the weights are computed as:

$$w_{rc}(i,j) = \frac{l_{rc}(i,j)}{l_{rc}(i,j) + l_{cr}(i,j)}, \tag{12}$$

$$w_{cr}(i,j) = \frac{l_{cr}(i,j)}{l_{rc}(i,j) + l_{cr}(i,j)}. \tag{13}$$

where $l_{rc}(i,j)$ and $l_{cr}(i,j)$ respectively denote the number of filter taps used for the point estimation of each image pixel of $\hat{x}_{rc}(i,j)$ and $\hat{x}_{cr}(i,j)$. The motivation for the second set of the weighting factors comes from the fact that the image pixel estimate obtained by the LPA filter with larger number of filter taps can be considered to be more accurate and reliable, hence such an estimate will have a larger weight and it will contribute more to the final estimate. The used weighting factors are inversely proportional to the estimation variances (Katkovnik, 1999).

5. Experimental Results and Discussion

We have used two 256×256 test images, *Rectangles* and *Stains* (Figs. 2(a) and 2(b)). The *Rectangles* image contains overlapping grayscale rectangles of different sizes, while the *Stains* image contains grayscale regions of irregular shapes. The parts of those images, both corrupted with zero mean additive white Gaussian noise with $\sigma_n = 20$ are shown in Figs. 3(b) and 4(b), respectively. The filters used in this paper are zero-order LPA based filters with the number of taps being determined by the RICI rule for each pixel independently. Rectangular windows are used in the kernel design. The filter supports were allowed to grow independently to the left-hand and to the right-hand side from the estimated signal sample, hence allowing to have asymmetrical estimation regions. Due to the central limit theorem, this results in larger filter supports and more precise estimates of the noise free pixel value. The pixel estimate is obtained using the filter whose support is the union of the two obtained subsupports (on the left hand side and the right hand side to the considered pixel). Note that, as in Lerga *et al.* (2008), in the presented results we have used $\Gamma = 4.4$ and $R_c = 0.85$.

The RICI rule, as described in Section 3, introduces a sequence of increasing filter supports. For each pixel value of the considered noisy image row (column), a sequence of confidence intervals is calculated using each of the filter supports from a set of increasing supports. Next, the algorithm tracks the intersection of confidence intervals and the amount of their intersection in order to find a proper filter support for the considered pixel as the largest one satisfying (3) and (4). The procedure is repeated for each image pixel, resulting in the image denoised by rows (columns). The same denoising procedure is then

Fig. 2. Noise-free 256×256 test images. (a) *Rectangles* image. (b) *Stains* image.

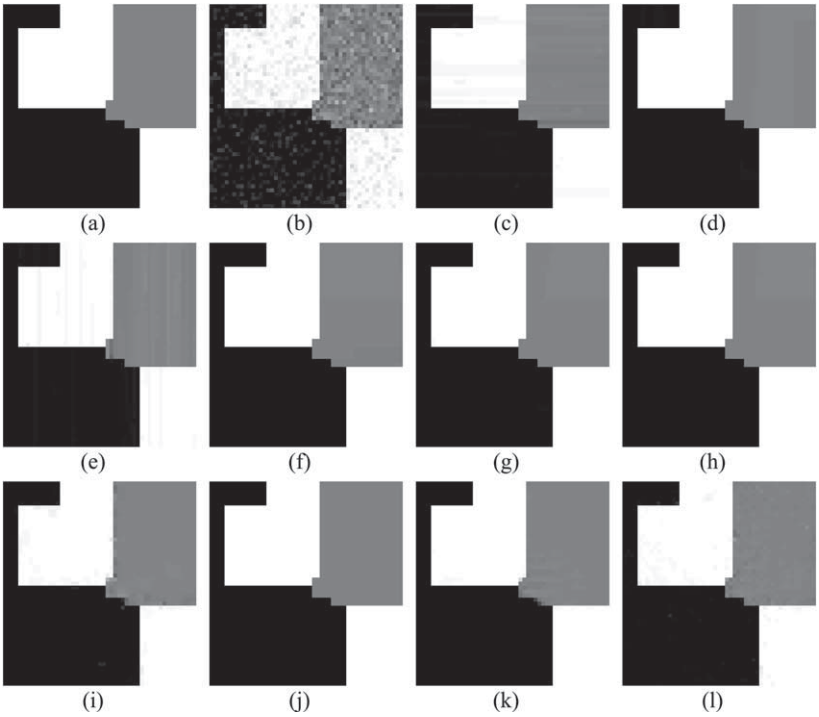

Fig. 3. Segment of the 256×256 *Rectangles* image. (a) Noise-free image. (b) Noisy image with zero-mean AWGN with $\sigma_n = 20$ (PSNR $= 22.08$ dB). (c) Image $\hat{x}_r(i,j)$ (PSNR $= 35.98$ dB). (d) Image $\hat{x}_{rc}(i,j)$ (PSNR $= 40.14$ dB). (e) Image $\hat{x}_c(i,j)$ (PSNR $= 35.99$ dB). (f) Image $\hat{x}_{cr}(i,j)$ (PSNR $= 40.39$ dB). (g) Final estimated image calculated using fixed weights (PSNR $= 41.32$ dB). (h) Final estimated image calculated using variable weights (PSNR $= 41.30$ dB). (i) Image denoised using undecimated wavelet shrinkage (Haar wavelet, hard thresholding with the threshold $3.5 \times \sigma_n$ and 8 decomposition levels) (PSNR $= 37.14$ dB). (j) Image denoised using the BM3D algorithm (PSNR $= 41.08$ dB). (k) Image denoised using the SA-DCT algorithm (PSNR $= 40.94$ dB). (l) Image denoised using the LPA-ICI method (threshold $\Gamma = 1.05$) (PSNR $= 36.59$ dB).

applied on the obtained image, only this time denoising is done by columns (rows), resulting in two images needed for the final stage of the algorithm, in which the images are combined into one final denoised image.

Our proposed method is compared to the LPA-ICI method (with $\Gamma = 1.05$, belonging to the interval $(0.8, 1.5)$ shown to be optimal for the LPA-ICI method; Katkovnik, 1999), the SA-DCT method (Foi *et al.*, 2007), the BM3D algorithm (Dabov *et al.*, 2007), and the conventional undecimated wavelet shrinkage method (Coifman and Donoho, 1994). It was shown in Foi *et al.* (2007) and Dabov *et al.* (2007), see also `http://www.cs.tut.fi/~foi/GCF-BM3D/` for additional results that the BM3D and SA-DCT methods outperform many other popular denoising methods, such as BLS-GSM (Portilla *et al.*, 2003), the patch-based method (Kervrann and Boulanger, 2006), MGGD (Cho and Bui, 2005), or the recursive anisotropic LPA-ICI method (Foi *et al.*, 2004).

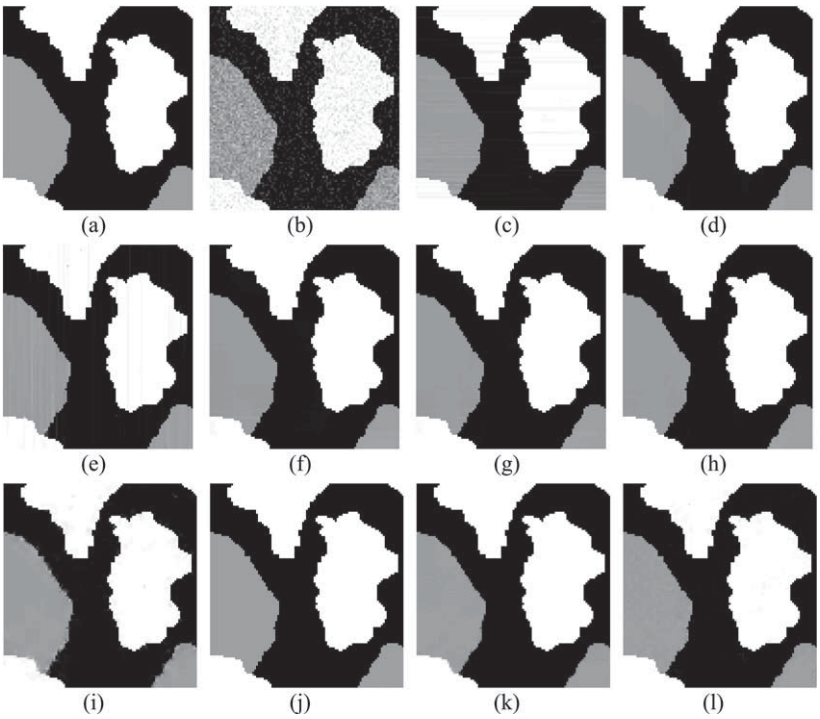

Fig. 4. Segment of the 256×256 *Stains* image. (a) Noise-free image. (b) Noisy image with zero-mean AWGN with $\sigma_n = 20$ (PSNR $= 22.08$ dB). (c) Image $\hat{x}_r(i,j)$ (PSNR $= 35.53$ dB). (d) Image $\hat{x}_{rc}(i,j)$ (PSNR $= 38.73$ dB). (e) Image $\hat{x}_c(i,j)$ (PSNR $= 35.78$ dB). (f) Image $\hat{x}_{cr}(i,j)$ (PSNR $= 38.82$ dB). (g) Final estimated image calculated using fixed weights (PSNR $= 39.47$ dB). (h) Final estimated image calculated using variable weights (PSNR $= 39.30$ dB). (i) Image denoised using undecimated wavelet shrinkage (Haar wavelet, hard thresholding with the threshold $3.5 \times \sigma_n$ and 8 decomposition levels) (PSNR $= 31.89$ dB). (j) Image denoised using the BM3D algorithm (PSNR $= 34.07$ dB). (k) Image denoised using the SA-DCT algorithm (PSNR $= 37.36$ dB). (l) Image denoised using the LPA-ICI method (threshold $\Gamma = 1.05$) (PSNR $= 37.17$ dB).

A segment of the image $\hat{x}_r$ (of the *Rectangles* and *Stains* test images) obtained in the first stage of the proposed algorithm is shown in Figs. 3(c) and 4(c). The algorithm has reduced the noise in the input noisy image, however some artifacts have been introduced in the horizontal direction. A segment of the image $\hat{x}_{rc}$, shown in Figs. 3(d) and 4(d), has the noise and the horizontal artifacts further reduced.

Figures 3(e), 3(f), 4(e) and 4(f) show the parts of the images $\hat{x}_c$ and $\hat{x}_{cr}$ obtained in the second stage of the algorithm. Unlike $\hat{x}_r$ which has artifacts in the horizontal direction, $\hat{x}_c$ has artifacts in the vertical direction, which get reduced in the image $\hat{x}_{cr}$.

Figures 3(g), 3(h), 4(g) and 4(h) show the segments of the final images obtained with the fixed and adaptive weights, respectively. In both cases, the undesirable visual artifacts are significantly reduced and the PSNR is increased.

Figure 5 presents the PSNR results as a function of σ_n for the *Rectangles* and *Stains* images. It can be seen that for small to medium σ_n values the proposed method out-

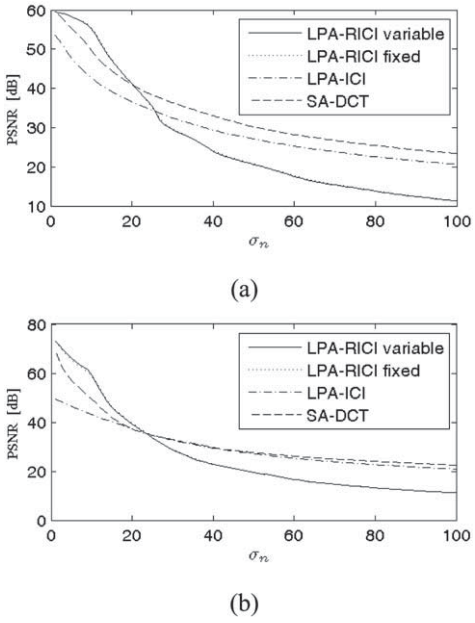

Fig. 5. PSNR as a function of σ_n for different denoising methods. (a) *Rectangles* image. (b) *Stains* image.

performs other considered denoising methods in terms of PSNR, even outperforming the state-of-the-art SA-DCT method (Figs. 3(k) and 4(k)), the LPA-ICI method (Figs. 3(l) and 4(l)), and the BM3D algorithm (Figs. 3(j) and 4(j)), as well as the undecimated wavelet shrinkage with Haar wavelet and hard thresholding (Figs. 3(i) and 4(i)).

The PSNR results for the *Rectangles* and *Stains* images are summarized in Tables 1 and 2 respectively. The second column of the tables gives PSNR of the noisy image, while the third column gives PSNR of the image denoised using the undecimated wavelets (Haar wavelet, hard thresholding with the threshold set to $3.5 \times \sigma_n$ and with 8 decomposition levels). The fourth and fifth columns are PSNRs for images denoised using the BM3D method and the SA-DCT method, respectively. The sixth column gives PSNR for the two images denoised using the anisotropic LPA-ICI method. The last two columns of the tables are the PSNR results obtained with the here-proposed algorithm with the fixed and variable weights, respectively.

As it can be seen from Tables 1 and 2, the newly developed LPA-RICI algorithm outperforms all of the considered methods for small to medium ($\sigma_n \leqslant 20$) noise deviations when applied to images that are piecewise constant along their rows and columns (such as the test images used in this paper). Also, unlike any of the other considered methods, our method uses 1D image processing, making it much simpler and computationally less complex. Note that in the case of larger σ_n values, the image property of being piecewise constant becomes significantly disturbed, hence resulting in lower PSNRs than those obtained by the SA-DCT method, the anisotropic LPA-ICI method or the BM3D algorithm, which, on the other hand, use computationally more demanding 2D approaches.

Table 1
Rectangles image PSNR obtained by different denoising methods

σ_n	Noisy image	Wavelets	BM3D	SA DCT	LPA ICI	LPA RICI fixed	LPA RICI variable
5	34.12	49.85	52.87	55.38	47.90	58.21	**58.25**
10	28.10	43.87	47.29	49.70	42.64	**55.48**	55.21
15	24.58	40.02	43.61	44.52	39.21	**47.44**	47.28
20	22.08	37.14	41.08	40.94	36.59	**41.32**	41.30
25	20.14	34.62	**38.97**	38.39	34.40	35.35	35.48
30	18.56	32.27	**37.43**	36.38	32.52	29.79	29.50
50	14.12	26.71	29.95	**30.24**	27.06	20.67	20.62
75	10.60	22.70	**27.07**	26.06	23.19	14.63	14.56
100	8.10	20.82	**24.60**	23.37	20.64	11.32	11.32

Table 2
Stains image PSNR obtained by different denoising methods

σ_n	Noisy image	Wavelets	BM3D	SA DCT	LPA ICI	LPA RICI fixed	LPA RICI variable
5	34.12	47.02	47.27	57.05	46.53	65.35	**66.11**
10	28.10	40.23	40.87	49.41	43.05	58.90	**59.09**
15	24.58	35.11	36.87	41.95	40.12	**46.35**	46.07
20	22.08	31.89	34.07	37.36	37.17	**39.47**	39.30
25	20.14	29.81	32.00	34.71	**34.74**	33.74	33.56
30	18.56	27.80	30.60	**32.83**	32.65	28.95	28.84
50	14.12	23.57	24.21	**27.61**	27.17	19.56	19.59
75	10.60	20.90	22.39	**24.51**	23.23	13.90	13.92
100	8.10	19.26	21.14	**22.47**	20.88	11.16	11.19

6. Conclusions

In this paper we have proposed a new algorithm for image denoising which is based on the LPA-RICI method. It uses the LPA-based filters and the RICI rule for their support selection. This three-stage algorithm is based on separable row-wise and column-wise pixel processing (meaning that denoising was done independently by rows and by columns), resulting in the final image whose significant features are well preserved, and with the noise being well suppressed not only in the homogeneous regions but in the areas around the edges as well.

Due to its separable nature, the first and the second stage of the algorithm are performed simultaneously, hence making it computationally more efficient, the efficiency being even further improved by having all image rows and columns denoised simultaneously.

The obtained results are compared with the current state-of-the-art methods for removing additive white Gaussian noise from images. It was shown that the proposed method outperforms other considered image denoising methods for small to medium noise levels and for images that are piecewise constant along their rows and columns. For other types of images and larger σ_n values two-dimensional anisotropic LPA-RICI method would have to be considered, which is the topic of our ongoing research.

Acknowledgements. This work is a part of the research project "Optimization and Design of Time-Frequency Distributions" (number 069-0362214-1575), which is financially supported by the Ministry of Science, Education and Sports of the Republic of Croatia.

References

Ausbeck, P.J., Jr. (2000). The piecewise-constant image model. *Proceedings IEEE*, 88(11), 1779–1789.

Buades, A., Coll, B., Morel, J.M. (2004). On image denoising methods. *Technical Report 2004-15 CMLA*.

Cho, D., Bui, T.D. (2005). Multivariate statistical modeling for image denoising using wavelet transforms. *Signal Processing: Image Communication*, 20(1), 77–89.

Coifman, R.R., Donoho, D.L. (1994). Translation-invariant de-noising. In: *Wavelets and Statistics*, *Lecture Notes in Statistics*, Vol. 103. New York, Springer, pp.125–150.

Dabov, K., Foi, A., Katkovnik, V., Egiazarian, K. (2007). Image denoising by sparse 3d transform-domain collaborative filtering. *IEEE Transactions on Image Processing*, 16(8), 2080–2095.

Fan, J., Gijbels, I. (1996). *Local Polynomial Modeling and Its Application*. Chapman & Hall, London.

Foi, A., Katkovnik, V., Egiazarian, K., Astola, J. (2004). A noval anisotropic local polynomial estimator based on direcional multiscale optimizations. In: *Proceedings of the 6th IMA International Conference Mathematics in Signal Processing*, Circencester, U.K., pp. 79–82.

Foi, A., Katkovnik, V., Egiazarian, K. (2007). Pointwise shape-adaptive dct for high-quality denoising and deblocking of grayscale and color images. *IEEE Transactions on Image Processing*, 16(5), 1395–1411.

Katkovnik, V. (1999). A new method for varying adaptive bandwidth selection. *IEEE Transactions on Signal Processing*, 47(9), 2567–2571.

Katkovnik, V., Egiazarian, K., Astola, J. (2002). Adaptive window size image de-noising based on intersection of confidence intervals (ICI) rule. *Journal of Mathematical Imaging and Vision*, 16(3), 223–235.

Katkovnik, V., Foi, A., Egiazarian, K., Astola, J. (2004). Directional varying scale approximations for anisotropic signal processing. In: *Proc. of EUSIPCO*, Vienna, Austria, pp. 101–104.

Katkovnik, V., Egiazarian, K., Astola, J. (2006). *Local Approximation Techniques in Signal and Image Processing*, SPIE Press Monograph, Vol. PM157.

Kervrann, C., Boulanger, J. (2006). Optimal spatial adaptation for patch-based image denoising. *IEEE Transactions on Image Processing*, 15(10), 2866–2878.

Lerga, J., Vrankic, M., Sucic, V. (2008). A signal denoising method based on the improved ICI rule. *IEEE Signal Processing Letters*, 15, 601–604.

Motwani, M.C., Gadiya, M.C., Motwani, R.C. (2004). Survey of image denoising techniques. In *Proc. GSPx*, Santa Clara, CA.

Portilla, J., Strela, V., Wainwright, M., Simoncelli, E.P. (2003). Image denoising using scale mixtures of gaussians in the wavelet domain. *IEEE Transactions on Image Processing*, 12(11), 1338–1351.

Ruppert, D. (1997). Empirical-bias bandwidths for local polynomial nonparametric regression and density estimation. *JASA*, 92(439), 1049–1062.

Serackis, A., Navakauskas, D. (2010). Treatment of over-saturated protein spots in two-dimensional electrophoresis gel images. *Informatica*, 21(3), 409–424.

Tomic, M., Sersic, D., Vrankic, M. (2008). Edge-preserving adaptive wavelet denoising using ICI rule. *Electronics Letters*, 44(11), 698–699.

Wu, J., Ruan, Q., An, G. (2010). Exemplar-based image completion model employing PDE corrections. *Informatica*, 21(2), 259–276.

J. Lerga was born in Nova Gradiska, Croatia, in 1983. He received the BS degree in electrical engineering from the Faculty of Engineering, University of Rijeka, in 2006. He is currently on doctoral studies on the Faculty of Electrical Engineering and Computing, University of Zagreb. His current research interests include time-frequency signal analysis, image and video processing and statistical signal processing.

V. Sucic received the BS degree in electrical and computer engineering (with the first class honours) from the Queensland University of Technology, Brisbane, Australia, in 1998, and the doctor of philosophy degree from the same university in 2004. Since 2005, he has been with the Faculty of Engineering, University of Rijeka, Croatia, where he is the Signals and Systems Chair and the head of the Statistical Signal Analysis and Processing Lab. His main research interests are time-frequency signal analysis and statistical signal processing. Dr. Victor Sucic has authored over 20 research publications, including two book chapters and two papers in leading signal processing journals.

M. Vrankić received his diploma degree, as well as MS and PhD degrees from University of Zagreb, Faculty of Electrical Engineering and Computing. Since 1999. he has been with the Department of Electronic Systems and Information Processing, Faculty of Electrical Engineering and Computing, University of Zagreb, Croatia. Since 2003 he has been with the Faculty of Engineering, University of Rijeka, Croatia, where he is currently assistant professor.

Separabilus skaitmeninių vaizdų triukšmo mažinimas grįstas pasikliautinų intervalų santykine sankirtos taisykle

Jonatan LERGA, Victor SUCIC, Miroslav VRANKIĆ

Šiame straipsnyje autoriai pristato naują metodą skaitmeninio vaizdo triukšmams šalinti. Metodas apjungia lokalią polinominę aproksimaciją (LPA) ir pasikliautinų intervalų santykinę sankirtos (RICI) taisyklę. Siūlomas algoritmas šalina triukšmą atskirai skaitmeninio vaizdo eilutėse ir stulpeliuose bei vėliau apjungia apdorojimo rezultatus į naują skaitmeninį vaizdą. Šiame straipsnyje pristatomo metodo rezultatas, signalo atsako į triukšmą (PSNR) prasme, yra labai panašus į neseniai mokslinėje spaudoje paskelbtų algoritmų rezultatus ir juos lenkia, kada triukšmo išsibarstymas yra mažas ar vidutinis vaizdo vietose kuriose taškų intensyvumas kinta labai nežymiai.